Original Research

Microencapsulation of porcine thyroid cell organoids within a polymer microcapsule construct

Yipeng Yang[1,2], Emmanuel C Opara[2], Yingbin Liu[1], Anthony Atala[2] and Weixin Zhao[2,3]

[1]General Surgery Department and Laboratory of General Surgery, Xinhua Hospital of Shanghai Jiao Tong University School of Medicine, Shanghai 200092, China; [2]Wake Forest Institute for Regenerative Medicine, Wake Forest School of Medicine, Medical Center Boulevard, Winston Salem, NC 27157, USA; [3]Co-Innovation Center of Neuro-regeneration, Nantong University, Nantong 226001, China
Corresponding authors: Anthony Atala. Email: aatala@wakehealth.edu; Weixin Zhao. Email: wezhao@wakehealth.edu

Abstract

Hypothyroidism is a common condition of hormone deficiency, and oral administration of thyroid hormones is currently the only available treatment option. However, there are some disadvantages with this treatment modality including compliance challenges to patients. Therefore, a physiologically based alternative therapy for hypothyroidism with little or no side-effects is needed. In this study, we have developed a method for microencapsulating porcine thyroid cells as a thyroid hormone replacement approach. The hybrid wall of the polymer microcapsules permits thyroid hormone release while preventing immunoglobulin antibodies from entry. This strategy could potentially enable implantation of the microcapsule organoids containing allogeneic or xenogeneic thyroid cells to secret hormones over time without the need for immunosuppression of recipients. Porcine thyroid cells were isolated and encapsulated in alginate-poly-L-ornithine-alginate microcapsules using a microfluidic device. The porcine thyroid cells formed three-dimensional follicular spheres in the microcapsules with decent cell viability and proliferation. Thyroxine release from the encapsulated cells was higher than from unencapsulated cells ($P < 0.05$) and was maintained during the entire duration of experiment (>28 days). These results suggest that the microencapsulated thyroid cell organoids may have the potential to be used for therapy and/or drug screening.

Keywords: Microencapsulation, organoids, thyroid, hormone deficiency, therapy

***Experimental Biology and Medicine* 2017; 242: 286–296. DOI: 10.1177/1535370216673746**

Introduction

Hypothyroidism is one of the most common forms of hormone deficiency which can be caused by many etiological factors,[1–3] including iodine deficiency, radioiodine therapy, thyroid resection, TSH-releasing disorder, and certain drugs such as tyrosine kinase inhibitors, rifampin, glucocorticoids, and colestipol.[4–6] The insufficient thyroid hormone status may slow life-sustaining processes of the body that result in dysfunction of tissues and organs, as well other life-threatening complications. Although current treatment of hypothyroidism by oral hormone administration is relatively simple and inexpensive, it is difficult to use to maintain the complex homeostatic interactions of hormones. Side-effects such as osteoporosis and cardiac toxicity often occur even with the most commonly used drug, levothyroxine sodium.[7] Transplantation of thyroid cells would be a more physiological alternative treatment for this endocrine disorder. However, immune rejection makes allogeneic and xenogeneic implants challenging. Immune isolation of cells via microencapsulation has been investigated for many years.[8,9] When cells are encased within a semipermeable hydrogel which hinders the larger host immune responders such as lymphocytes, immunoglobulins, and antibodies from penetrating into the microcapsules, the encapsulated cells are insulated from the immune system of the host's body.[10] On the other hand, the passage of small molecules such as nutrients, oxygen, electrolytes, hormones, and metabolites are permitted. Cell encapsulation technology has been used in some cells, such as islet cells,[11,12] parathyroid cells,[13,14] liver cells,[15] Leydig Cells,[16] ovarian cells,[17] and others.[18] However, microencapsulation of thyroid cells has not been reported. Using a three-dimensional (3D) microfluidic device[19] and polymer biomaterials, we have developed microencapsulated organoid constructs of porcine thyroid cells which closely resemble the thyroid gland in both morphology and function. The viability, proliferation, and hormonal secretion of the encapsulated porcine thyroid cells were evaluated *in vitro*. Our present study shows that encapsulated thyrocytes could form functional cell follicular structures and maintain viability and hormone release *in vitro* for at least 28 days.

Materials and methods

Materials

RPMI-1640 medium, PBS, and HBSS (with and without Ca^{2+}) were purchased from HyClone (Logan, UT). Ultrapure low-viscosity-high-mannuronic-acid (LVM), ultra-pure sodium alginate (20–200 mPas), and low-viscosity-high-guluronic-acid alginate (LVG; 20–200 mPas) were purchased from Nova-Matrix, (Sandvika, Norway), Poly-L-ornithine hydrochloride (PLO, MW = 15,000–30,000; Sigma-Aldrich, St. Louis, MO) and sodium citrate (Fisher Scientific, Fair Lawn, NJ) were dissolved in Eagle minimum essential medium (M0518; Sigma-Aldrich). The molecular weights of LVM and LVG were 75–200 kDa as reported by the manufacturer. The LVG/LVM ratios of $\leq$1 and $\geq$1.5 were used for LVG and LVM, respectively, in the experiments. Thyrotropic hormone (TSH), calcium chloride, agar, Triton X-100 and FITC-dextran (avg MW = 40,000) were obtained from Sigma-Aldrich. Fetal bovine serum (FBS) was purchased from Gibco (Grand Island, NY).

Thyroid cell isolation and culture

Porcine thyroid glands were obtained from farm pigs and kept in cold HBSS. The glands were washed in 70% alcohol, and then washed three times with HBSS containing penicillin and streptomycin (HBSS/PS) to remove blood cells and connective tissue. The gland tissue was finely minced and dissociated by incubating in enzyme mixture of 50 U/mL collagenase 2 (Worthington, Lakewood, NJ) and 1 mg/mL dispase (grade II; Roche, Indianapolis, IN) at 37°C with intermittent gentle agitation. The supernatant containing suspended follicles and cells was transferred to a centrifuge tube every half hour, and fresh enzyme mixture was added to the remaining undigested tissue fragments. The above procedure was repeated six to nine times. The same volume of FBS was added to the supernatants to stop digestion, and the follicles were allowed to settle by gravity sedimentation on ice for 1 h. The digestion process usually lasted for 3–5 h until no more tissue remained visually. After removing the supernatant, the pellets were resuspended in the growth medium (GM) composed of RPMI-1640 containing 10% FBS and 1 mU/mL thyrotropic hormone). After pooling and rinsing three times by centrifugation (200 *g*; 5 min), the resultant pellets were resuspended in the GM and passed through a 100 μm mesh cell strainer. The follicles and cells were seeded on 24-well cell culture plates for morphology observation and Petri dishes coated with 2% agar for microencapsultion in GM. The plates and dishes were incubated at 37°C in a standard humidified 5% CO_2 atmosphere.

Thyroid cell characterization

After incubation of cells on chamber slides for two days, characterization by immuno-fluorescence staining was performed. After fixing and permeabilizing, the samples were blocked in a serum-free protein block (Dako). The samples were incubated in a solution made up of a mixture of goat anti-Tg (Santa Cruz Biotechnology, CA) and rabbit anti-NIS (Santa Cruz Biotechnology, CA) at 4°C overnight. The cells were then incubated with a mixed solution of donkey anti-goat IgG (Alexa Fluor® 594-conjugated; Invitrogen, Grand Island, NY) and donkey antirabbit IgG (Alexa Fluor® 488-conjugated; Invitrogen) for 60 min in the dark. Next, a mounting medium for fluorescence with DAPI (Vectashield, Burlingame, CA) was used to counterstain the nucleus. The negative controls were incubated with only secondary antibodies. Images were taken using a fluorescence microscope (Leica DM4000B).

Microencapsulation procedure

Microencapsulation of thyroid cells was performed using a newly designed 8-nozzle microfluidic device as previously described.[17] This microencapsulation system is regarded to be efficient and advanced, and the design, principle and assessment have been demonstrated in our previous study.[19] After culturing for seven days, the thyroid cells were pelleted by centrifugation (200 *g*; 5 min) and dispersed using 200 μl pipette tips. An aliquot of the cells was directly seeded in 24-well plates (1×10^5 cells/well) in the growth medium as unencapsulated controls. The cells for encapsulation were suspended in 1% (w/v) ultrapure LVM alginate solution (3×10^6 cells/mL) and loaded in a syringe, which was connected to the 8-nozzle microfluidic device. With the pump speed at 0.9 ml/min and the high-throughput air flow at 3.6 psi, the microbeads were formed and collected in 1.1% calcium chloride solution and allowed a 15-min crosslinking time. Following two washes with HBSS (without calcium), the microspheres were incubated in 0.1% (w/v) PLO for 30 min to form a semipermeable coating to achieve appropriate permeability. The microcapsules were then incubated in 55 mM sodium citrate solution for 4 min to liquefy the inner cell-containing alginate core. The PLO-coated microbeads were washed twice and incubated in 1.25% (w/v) ultrapure LVG alginate solution for 5 min at 4°C to form the final outer layer resulting in alginate-PLO-alginate (APA) microcapsules followed by three washes with HBSS (with calcium) that initiate crosslink of the outer layer (Figure 1). The microencapsulated thyroid cell organoids were cultured in 24-well plates (130 beads/well) at 37°C in a humidified 5% CO_2 atmosphere.

To characterize the permeability of the microcapsules, blank beads in a PBS solution containing FITC-dextran (MW = 40 k; Sigma-Aldrich) or Alexa Fluor® 488-conjugated IgG (MW = 160 k; Invitrogen) were incubated for 48 h at 4°C under soft agitation. The images of the beads were then taken under a confocal laser-scanning microscope (Olympus FluoviewFV10i) used to examine fluorescence within them.

Morphological studies of the microcapsules

The shape and surface of APA microcapsule organoids were examined under bright-field microscope (Zeiss Axiovert 200 M) and scanning electron microscopy (SEM; Hitachi S-2600N). Briefly, the microbeads were collected and fixed in 2.5% SEM-grade glutaraldehyde solution in PBS for 2 h. Then, the samples were rinsed in running DI water and dehydrated in graded alcohol concentrations.

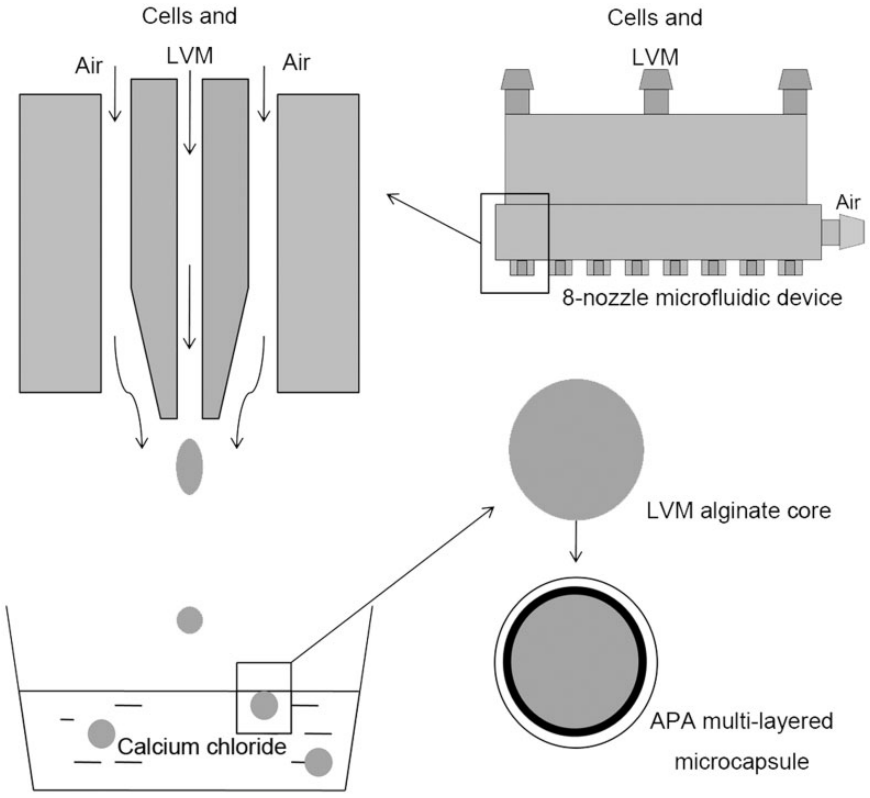

Figure 1 Schematic of the microencapsulation process. The cells were suspended in LVM solution and the inner alginate core was formed by the 8-nozzle microfluidic device. After cross-linking in calcium chloride solution, the inner core was coated with PLO and then LVG to form the APA multilayered microcapsule.

After air drying, the samples were mounted on an SEM stand, sputter coated and observed with a Hitachi S-2600N scanning electron microscope.

Viability and proliferation analysis

To assess the viability of encapsulated thyroid cells, we performed live and dead staining as previously described.[17] Briefly, cell-containing microcapsules were transferred to a 1.5 ml brown (light blocking) Eppendorf tube every four days. The collected microcapsules were incubated in 25 μM CFDA SE (carboxyfluoresceindiacetate, succinimidyl ester; Invitrogen, Grand Island, NY) for 15 min at 37°C. They were then incubated in growth medium with 10% FBS for 30 min. This was followed by incubation in 50 μg/ml of propidium iodide (PI; Invitrogen) for 2 min. After washing with HBSS and fixing with 4% paraformaldehyde, the samples were observed using the fluorescence microscope (Leica DM4000B) for live/dead evaluation. The proliferation of microencapsulated porcine thyroid cells was evaluated using MTS assay (CellTiter 96$^{@}$AQ$_{ueous}$ One Solution, Promega, Madison, WI) according to the manufacturer's instruction at the different time points. After recording the absorbance at 490 nm using a 24-well plate reader, the cell number of the samples was measured based on a standard curve and expressed as cell number/well for the microencapsulated cells and the control unencapsulated cells under a monolayer culture.

Immuno-fluorescence staining

After 20 days' incubation, 30 microcapsules were collected for frozen sectioning. After washing with PBS, the microcapsules were embedded in FSC22 clear frozen section compound (Leica Biosystems, Richmond, IL). Frozen sections (6 μm thick) of the microcapsules were sectioned using a cryostat (Leica CM 1950) and mounted on slides. After fixing in acetone and protein blocking, the slices were incubated in the primary antibody of goat anti-Tg (Santa Cruz Biotechnology), rabbit anti-NIS (Santa Cruz Biotechnology) and mouse antithyroxine (GenWay, San Diego, CA) at room temperature for 1.5 h in a humidified chamber. Following washing with PBS, the slices were incubated with secondary antibodies of donkey antigoat IgG (Alexa Fluor® 594-conjugated; Invitrogen), and donkey antirabbit IgG (Alexa Fluor® 488-conjugated; Invitrogen), and goat antimouse IgG (Alexa Fluor® 594-conjugated; Invitrogen) for 30 min at room temperature in the humidified chamber. After nucleus counterstain and mounting, the slices were evaluated by a fluorescence microscope (Leica DM4000B).

Measurement of thyroid hormone release

To evaluate endocrine functions from microencapsulated and unencapsulated monolayer porcine thyroid cells, the levels of thyroxine in the culture medium were measured. Both encapsulated and unencapsulated cells were cultured in 24-multiwell plates in the growth medium for

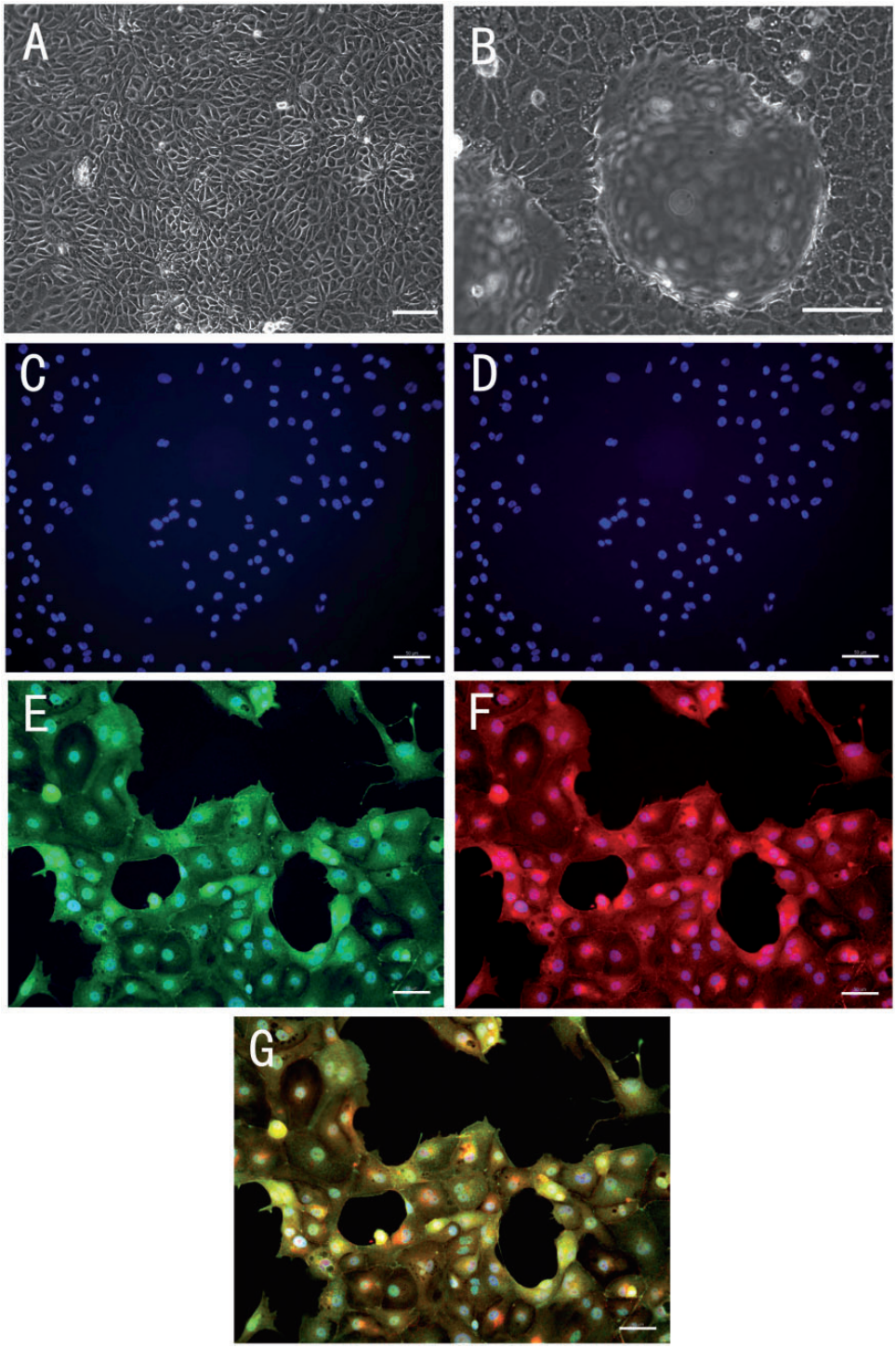

Figure 2 Representative images of light microscopic observation and immuno-fluorescence staining of primary cultured porcine thyroid cells. (a) The monolayer porcine thyroid cells in culture after two days of incubation. (b) The thyroid cells with the hemisphere-like domes formed in culture after four days of incubation. (a and b) Scale bar = 100 μm. (c) Negative control for antirabbit IgG. (d) Negative control for antigoat IgG. (e) Positive staining of sodium-iodide symporter (NIS). (f) Positive staining of thyroglobulin (Tg). (g) Composite picture of NIS, Tg, and DAPI. (c to g) Scale bar = 50 μm. (A color version of this figure is available in the online journal.)

28 days, and conditioned medium was collected once every four days. The measurements of thyroxine were carried out using ELISA kits (L140928892; Biomatik, Wilmington, DE). The hormone concentrations of the samples were read off a standardized curve and expressed as ng/cell/24 h.

Data analyses

Statistical analysis was performed using SPSS (v 19.0). All values are expressed as mean ± standard deviation. The Student t-test was used to compare the two groups. After statistical analyses, the differences were considered to be significant when $P \leq 0.05$.

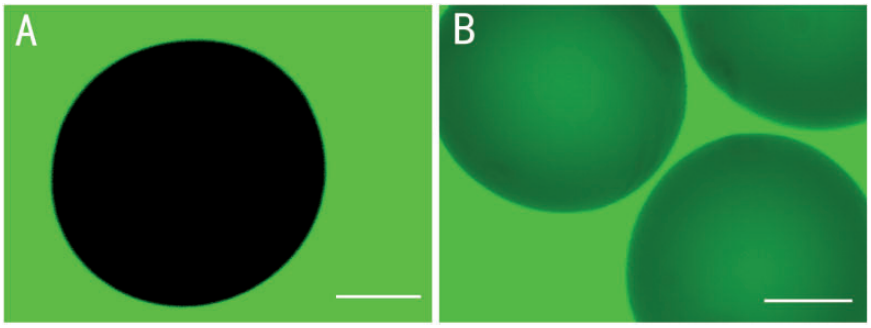

Figure 3 Representative images of the beads taken by confocal laser-scanning microscope. (a) No fluorescence could be observed inside the beads when incubated with Alexa Fluor® 488-conjugated IgG (160 kDa) for 48 h. (b) Fluorescence was observed in the beads when incubated with FITC-dextran (40 kDa). Thus molecules which are smaller than dextran (40 kDa) can pass through the capsule membrane, but those as large as IgG (160 kDa) cannot pass through the capsule membrane. (A color version of this figure is available in the online journal.)

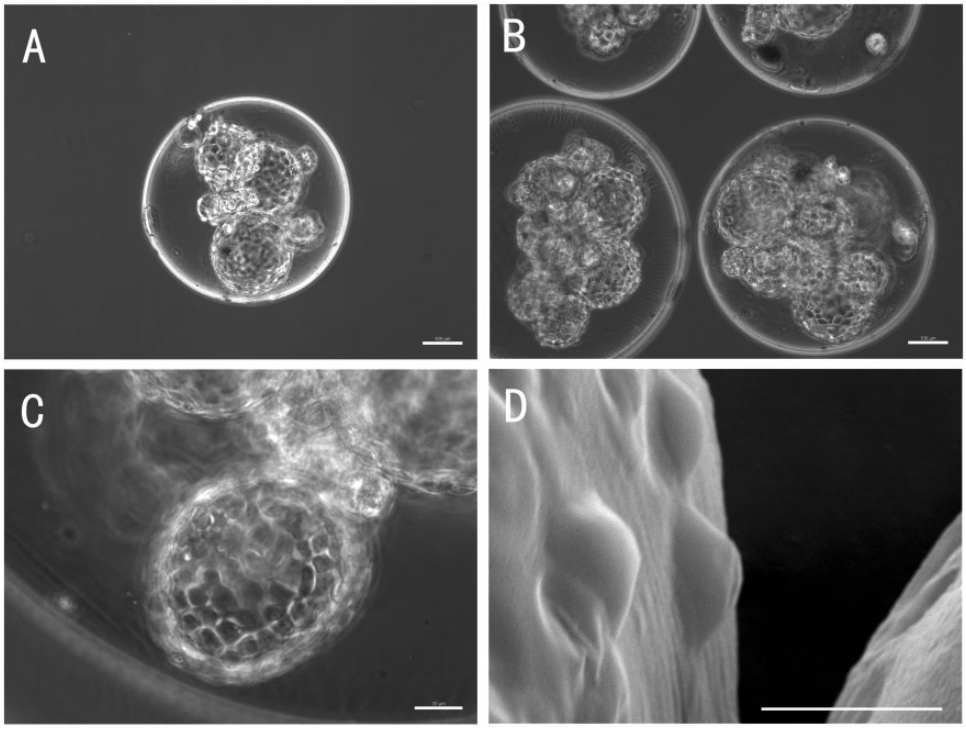

Figure 4 Morphology of the microcapsules at 20 days after encapsulation: The representative images show that the APA microcapsules are spherically shaped and the cell follicular structures can be seen within the microcapsules. (a) A typical microcapsule containing three-dimensional spheres of cells (100×). The scale bar on the image depicts 100 μm. (b) Image showing that the beads contained spherical cell structures (100×). The scale bar on the image depicts 100 μm. (c) Magnified image of one sphere of thyroid cells in the microcapsule (400×). The scale bar on the image depicts 30 μm. (d) Representative SEM image showing a smooth and intact capsule surface (1800×). The scale bar on the image depicts 25 μm

Results

Morphology and characterization of cultured porcine thyroid cells

The morphology of porcine thyroid cells was observed under the light microscope. The monolayer glandular epithelial cells covered the culture dish completely after two to three days (Figure 2(a)). After four days, the appearance of typical hemisphere-like domes was observed (Figure 2(b)). Before encapsulation, the cultured cells were screened for the expression of sodium-iodide symporter (NIS) and thyroglobulin (Tg) by immuno-fluorescence staining. Thyroglobulin is a large precursor of thyroid hormones and iodinated at tyrosine residues. NIS mediates active iodide transport in thyroid hormone synthesis. Tg and NIS are considered as specific markers for thyroid cells.[20] The cultured cells stained positively for both Tg and NIS (Figure 2).

Permeability and morphology of the microcapsule organoids

Using imaging technique and fluorescence intensity profile analysis, we have previously demonstrated the multilayer microcapsule system,[21] which we have used here to micro-encapsulate porcine thyroid cells. Permeability properties

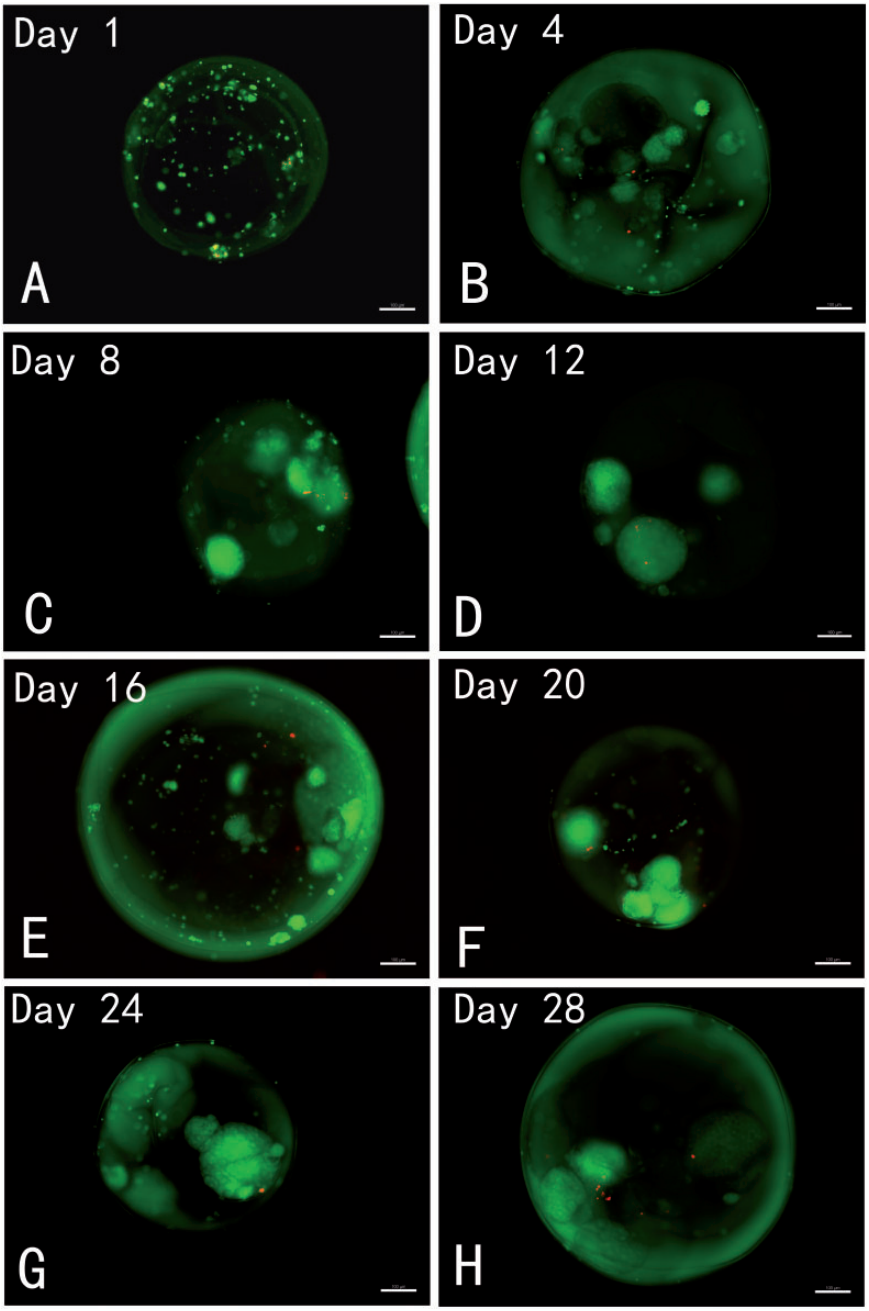

Figure 5 Representative images of live/dead staining of encapsulated porcine thyroid cells with CFDA/PI dyes at designated time points: The live cells are represented by the green fluorescence of CFDA, and the dead cells are indicated by red fluorescence of PI. All images show good viability of the encapsulated cells throughout the various time points. The encapsulated thyroid cells formed spherical structures which were maintained during the experimental period with good viability. Scale bar on the images depict 100 μm. (A color version of this figure is available in the online journal.)

of the microcapsule membrane are key to the immune insulation and therapeutic efficacy of the implanted microbeads. A successful semipermeable microcapsule membrane for the thyroid cells should allow the diffusion of thyroid hormones (MW = 600–800), thyroid-stimulating hormone (MW = 28,000), nutrients, oxygen, electrolytes and wastes, while blocking immunoglobulins, antibodies and host cells which mediate immune response. We chose FITC-dextran (MW = 40 k) or Alexa Fluor® 488-conjugated IgG (MW = 160 k) to test the permeability of the capsule and assess the suitability of the alginate-PLO-alginate microcapsules for encapsulating thyroid cells. Figure 3 shows that dextran (MW = 40 k) diffused through the capsule membrane and could be seen in the beads, while IgG was hindered from transport into the microbeads. This result is consistent with those from our previous studies of the permeability properties of APA microcapsules,[21,22] and suggests that this APA microcapsule can be used for thyroid cell encapsulation as an immunoisolation strategy in therapy. Under light microscope, the APA microcapsules exhibited a regular round shape with relatively uniform size range (Figure 4(a)). The cells and 3D structures can be

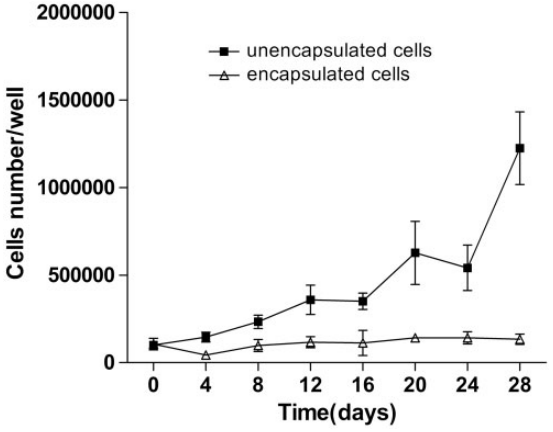

Figure 6 The proliferation of encapsulated and unencapsulated porcine thyroid cells: The cells in both groups were cultured in 24-well plates with growth medium, and cell growth rates were evaluated by the MTS assay at the indicated times. Data presented are means ± SD ($n = 6$ in each group). The results indicate that the proliferation of the unencapsulated cells was higher than that of encapsulated cells. The figure represented the data from one of two separate experiments

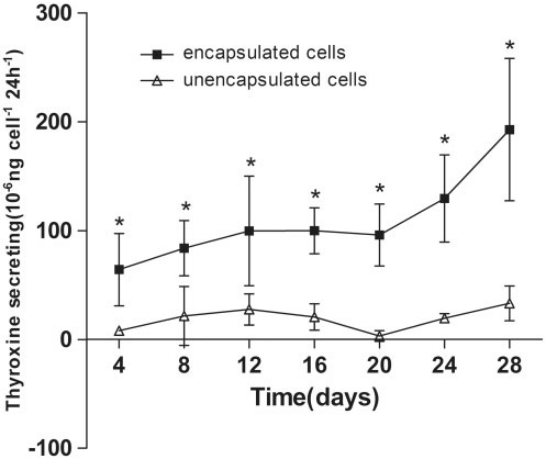

Figure 7 Thyroxine secretion by encapsulated and monolayer cultured porcine thyroid cells cultured for 28 days. Results are presented as means ± SD ($n = 6$ in each group). *denotes statistical significance ($P < 0.05$). The figure represented the data from one of two separate experiments

observed within the transparent microsphere (Figure 4(a) to (c)), and the spheres of porcine thyroid cells were observed in each microcapsule (Figure 4(b)). SEM images showed a smooth and complete external surface of the microbeads, which did not involve inner core cells (Figure 4(d)). In contrast to unencapsulated thyroid cells in 2D culture (Figure 2(b)), with stimulation by TSH, the encapsulated porcine thyroid cells gathered and formed 3D follicular spheres in the inner core of the liquefied alginate microcapsules within 48 h. The diameters of the hollow spheres of the thyroid cells were 80.2 ± 45.5 μm ($n = 50$), and 9.2 ± 5.5 ($n = 30$) spheres were observed in each microcapsule. The integrity of the structure was maintained for more than 28 days.

Viability and proliferation of the encapsulated porcine thyroid cells

Live and dead staining was used to assess cell viability. Figure 5 shows live and dead cells imaging in the representative samples of the microcapsules from day 1 to day 28. It can be seen that most of the encapsulated thyroid cells at each time point were viable with only a few dead cells inside the microcapsules. The viability of the cells in the microcapsules was maintained for at least 28 days in culture. It was observed that the encapsulated thyroid cells formed spherical structures which were maintained throughout the experiment with good viability. To quantitatively analyze the proliferation of encapsulated and unencapsulated thyroid cells, an MTS assay was conducted every four days according to the experimental protocol. We observed a low rate of proliferation of the encapsulated cells, but a rapid growth pattern from monolayer cultured thyroid cells (Figure 6).

Secretory function of the encapsulated porcine thyroid cells

To assess endocrine function, thyroxine release from porcine thyroid cells in monolayer culture and microcapsules was examined in complete growth medium at each time point. Hormone release could be seen in both encapsulated and unencapsulated thyroid cells starting from day 4 (Figure 7). Thyroxine secretion was significantly higher in encapsulated cells than in monolayer cultured cells at all time points ($P < 0.05$). The level of thyroxine released by microencapsulated thyroid cells continued to increase during 28 days (hormone release measurement shown in Figure 7). To further confirm the morphology of microbeads and the secretory function of the cell follicular structures in the microcapsule organoids, we collected the microbeads at day 20 and assessed the expression of NIS, Tg, and thyroxine by immunofluorescence staining in frozen sections. The functional thyroid follicle-like structures that were developed in the microcapsules stained positive for both NIS and Tg, which play important roles in thyroid hormone synthesis and a positive stain for the thyroid hormone, thyroxine, was also observed in the colloid inside the lumen of the follicular spheres (Figure 8).

Discussion

Hypothyroidism is one of the most common hormone deficiency problems. Because of the limitations of lifelong oral hormone administration for treating hypothyroidism, the applications of tissue engineering and regenerative medicine in thyroid hormone deficiency management are highly desirable. One approach has been to regenerate the thyroid gland using stem cells. *In vitro* thyroid-like cell differentiation from mouse embryonic stem cells (mESCs) was first demonstrated by Lin *et al*. in 2003.[20] Then, Arufe *et al*. reported the directed derivation from mESCs to thyroid follicular cells. TSH, insulin-like growth factor-1 (IGF-1), and insulin were essential for the differentiation to thyroid cells.[23,24] Subsequently, Antonica *et al*. implanted functional ESC-derived thyroid cells into mice to rescue hypothyroidism.[25] However, clinical application of ESC is restricted

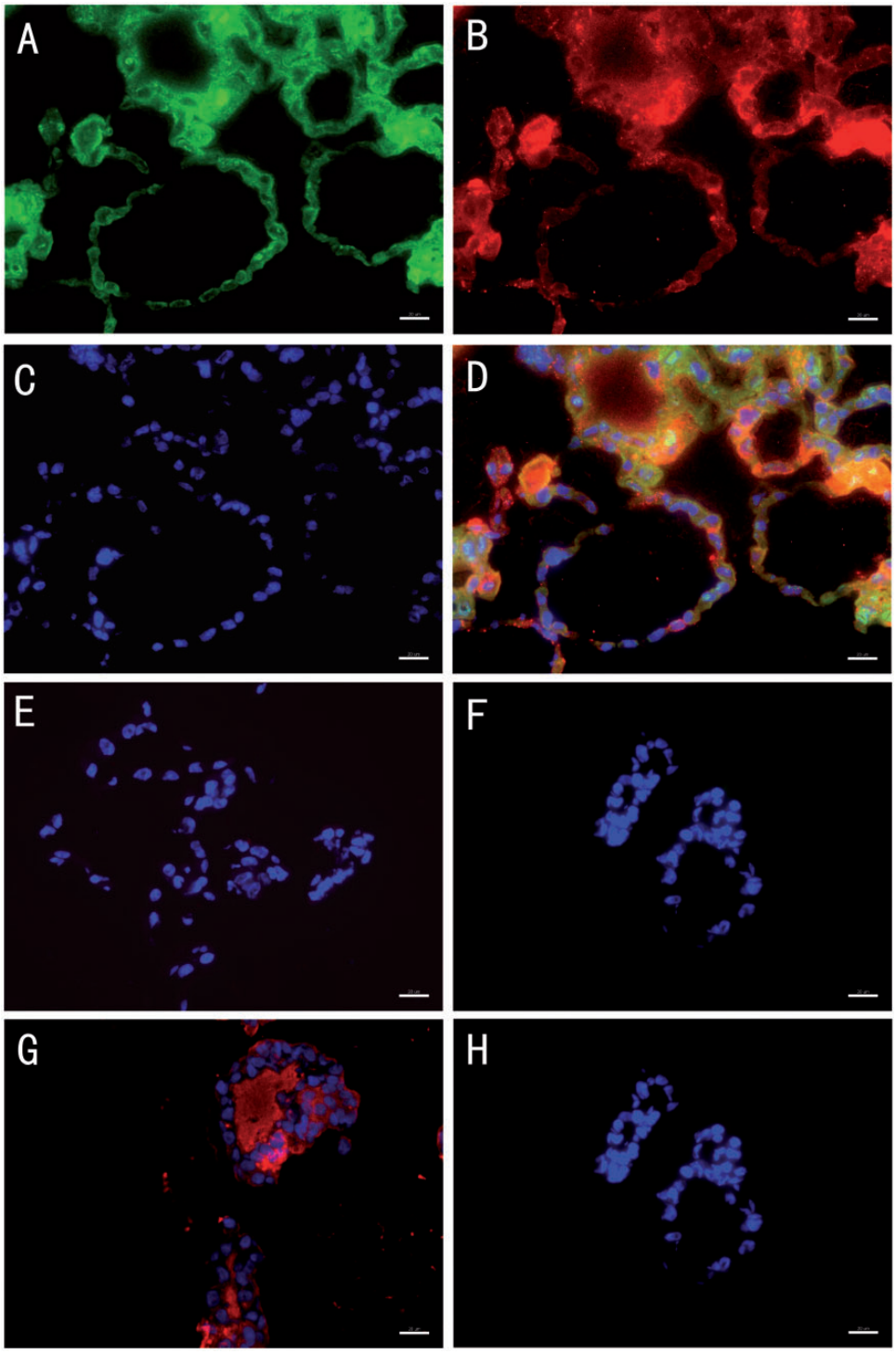

Figure 8 Representative images of immuno-fluorescence staining of the microbeads at day 20. The images show that there were cell follicular structures inside the microbeads, which stained positive for both sodium-iodide symporter (NIS) (a) and thyroglobulin (Tg) (b). Cells were stained with DAPI only (c). Composite image including NIS, Tg and DAPI (d). Negative control of antigoat IgG (e). Negative control of antirabbit IgG (f). Thyroxine was detected in the lumen of follicular spheres (g). Negative controls of antimouse IgG (h). Scale bars on the images depict 20 μm. (A color version of this figure is available in the online journal.)

because of its oncogenecity. Another approach is to fabricate thyroid tissue with allogenic or xenogeneic thyroid cells and biomaterials. Bell *et al*. reconstructed a gland-equivalent structure with thyroid cells, combined with fibroblasts and collagen gel *in vitro*, and the cells formed functional thyroid gland equivalents *in vivo* after implantation.[26] Toda *et al*. have also used a 3D culture technology to fabricate thyroid follicles from porcine thyroid cells.[27,28] Furthermore, Arauchi *et al*. used a cell sheet engineering method to form typical thyroid structures with hormone secretory function.[29] In these studies, although thyroid follicles were successfully reconstructed, graft

rejection after implantation was a major barrier to clinical application. In the present study, we have therefore adopted the approach of immunoisolation by microencapsulating porcine thyroid cells, as a strategy to overcome the immune rejection barrier, with the potential to expand the sources of cells that can be used for clinical application.

Microencapsulation has been applied in drug delivery, biosensors, bioanalyses, microelectronics, cell delivery, and cell transplantation.[30–32] The technique of cell microencapsulation for hormone replacement was first described by Lim and Sun for the encapsulation of pancreatic islets as a treatment option for insulin deficiency.[33] Many types of natural and synthetic biomaterials have since been explored for cell encapsulation, including alginate,[34] collagen,[35] hyaluronic acid (HA),[36] agarose,[37] gelatin,[38] polydimethylsiloxane (PDMS),[39] and tyramine.[40] In the present study, we chose ultrapure alginate because of several attractive properties, including improved biocompatibility, bioinertness, and lower biodegradability.[41] Alginate can form a gel with controllable gelation property under mild physiological conditions,[42] with tunable pore size to control the diffusion of biomolecules.[43,44] As a hydrogel, it can also provide a synthetic extracellular 3D environment which mimics certain beneficial properties of the extracellular matrix (ECM)[45] for cell growth.[46,47] It is noteworthy that in previous studies with alginate microcapsules, 1.5% alginate concentration was used for the fabrication of the inner alginate core.[10,17,18] In the present study for the thyroid cells, we used 1% LVM alginate, because it was found to generate a matrix that provided more suitable support for the formation of cell follicular structures and the controlled diffusion of nutrients and hormone products. This observation highlights the important relationship between matrix components and cell phenotype and function consistent with studies on other cell types.[48] Furthermore, the maintenance of good cell viability during the experimental period shown by the live/dead staining could be due to not only the favorable extracellular environment but also the integral follicular structure which provided connections and communications between the cells within the microcapsules.

To achieve the proper permeability, we used longer incubation time of alginate beads in PLO solution in order to increase the mechanical strength of the capsules and to potentially invoke less immunoreactions if implanted,[49] as previous studies by our group had shown that longer duration of PLO coating reduces the permeability of the beads.[22] In this study, we tested the permeability of microcapsules to determine if the multilayer microcapsules are appropriate for thyroid cell encapsulation. Our permeability test shows that TSH (MW = 28,000) is able to diffuse through the semipermeable microcapsule membrane and stimulate thyroid cells to release hormone that can exit, while large molecules such as IgG are excluded from entry.

It has previously been shown that several days after the formation of a monolayer, thyroid cells may partly lose TSH-binding capacity and the capacity to concentrate iodide.[50] In our study, we found that TSH stimulation did not induce thyrocytes in 2D culture to form cell follicular structures in contrast to the encapsulated cells. Although after microencapsulation the expansion of cells was much slower presumably because the space within the microcapsules was restricted when compared to the unencapsulated cells and the proliferation of thyroid cells would be very limited after the formation of the follicles,[51] the 3D environment of the microcapsules resulted in the maintenance of the follicular structures and hormone secretion for a longer period, showing the beneficial properties of this microenvironment in creating a suitable cell niche.

The result of ELISA test indicates that the reorganized cell follicular structures in the microcapsule organoids maintained better function with the release of thyroxine compared with monolayer cell cultures. The higher synthetic and secretory capability of encapsulated thyroid cells may be due to optimal development of follicular structures which are the functional units of the thyroid gland in 3D spheroids, as well as the favorable environment provided by the alginate hydrogel. In future studies, we will determine the regulation of the organoids by TSH in long-term experiments in order to monitor any temporal changes in morphological and functional properties dynamically, albeit, this APA microcapsule system has been shown to maintain durable mechanical strength and physical properties over time.[12] In addition, *in vivo* studies of the performance of these organoid constructs are also required.

Conclusion

We have successfully used the multilayer microcapsules[12,17,21] for encapsulating viable porcine thyroid cells. The 3D microencapsulated thyroid cell organoids maintained normal morphology, viability, and secretory function for at least 28 days. Our study, which is the first description of successful microencapsulation of thyroid cells, represents an important step toward the goal of tissue engineering of functional thyroid tissue for use as a more physiological alternative therapy for hypothyroidism, as well as for potentially screening drug efficacy on thyroid tissue.

Authors' contribution: All authors participated in the design, interpretation of the studies and analysis of the data and review of the manuscript; YY, WZ and ECM conducted the experiments and wrote the manuscript; AA and YL was responsible for the design of the study; WZ modified the study plan and controlled the data analyses; ECM and YL revised the manuscript.

ACKNOWLEDGEMENTS

We wish to thank Drs. John Patrick McQuilling and Sittadjody Sivanandane for technical guidance. This study was supported by a Translational Research Grant from the Department of Commerce, State of North Carolina (40065) and Skilled Personnel Research Plan of Xinhua Hospital, Shanghai Jiao Tong University School of Medicine.

DECLARATION OF CONFLICTING INTERESTS

The author(s) declared no potential conflicts of interest with respect to the research, authorship, and/or publication of this article.

REFERENCES

1. Hollowell JG, Staehling NW, Flanders WD, Hannon WH, Gunter EW, Spencer CA, Braverman LE. Serum TSH, T(4), and thyroid antibodies in the United States population (1988 to 1994): National Health and Nutrition Examination Survey (NHANES III). *J Clin Endocrinol Metab* 2002;**87**:489–99
2. McLachlan SM, Rapoport B. Why measure thyroglobulin autoantibodies rather than thyroid peroxidase autoantibodies? *Thyroid* 2004;**14**:510–20
3. Santini F, Marzullo P, Rotondi M, Ceccarini G, Pagano L, Ippolito S, Chiovato L, Biondi B. Mechanisms in endocrinology: the crosstalk between thyroid gland and adipose tissue: signal integration in health and disease. *Eur J Endocrinol* 2014;**171**:R137–52
4. Limonard EJ, Bisschop PH, Fliers E, Nieveen VDE. Thyroid function after subtotal thyroidectomy in patients with Graves' hyperthyroidism. *Sci World J* 2012;**2012**:548796
5. Lilley JS, Lomenick JP. Delayed diagnosis of hypothyroidism following excision of a thyroglossal duct cyst. *J Pediatr* 2013;**162**:427–28
6. Bonato C, Severino RF, Elnecave RH. Reduced thyroid volume and hypothyroidism in survivors of childhood cancer treated with radiotherapy. *J Pediatr Endocrinol Metab* 2008;**21**:943–49
7. Clarke N, Kabadi UM. Optimizing treatment of hypothyroidism. *Treat Endocrinol* 2004;**3**:217–21
8. Kang A, Park J, Ju J, Jeong GS, Lee SH. Cell encapsulation via microtechnologies. *Biomaterials* 2014;**35**:2651–63
9. Olabisi RM. Cell microencapsulation with synthetic polymers. *J Biomed Mater Res A* 2015;**103**:846–59
10. Fort A, Fort N, Ricordi C, Stabler CL. Biohybrid devices and encapsulation technologies for engineering a bioartificial pancreas. *Cell Transplant* 2008;**17**:997–1003
11. Vaithilingam V, Kollarikova G, Qi M, Lacik I, Oberholzer J, Guillemin GJ, Tuch BE. Effect of prolonged gelling time on the intrinsic properties of barium alginate microcapsules and its biocompatibility. *J Microencapsul* 2011;**28**:499–507
12. Pareta R, McQuilling JP, Sittadjody S, Jenkins R, Bowden S, Orlando G, Farney AC, Brey EM, Opara EC. Long-term function of islets encapsulated in a redesigned alginate microcapsule construct in omentum pouches of immune-competent diabetic rats. *Pancreas* 2014;**43**:605–13
13. Moskalenko V, Ulrichs K, Kerscher A, Blind E, Otto C, Hamelmann W, Demidchik Y, Timm S. Preoperative evaluation of microencapsulated human parathyroid tissue aids selection of the optimal bioartificial graft for human parathyroid allotransplantation. *Transpl Int* 2007;**20**:688–96
14. Picariello L, Benvenuti S, Recenti R, Formigli L, Falchetti A, Morelli A, Masi L, Tonelli F, Cicchi P, Brandi ML. Microencapsulation of human parathyroid cells: an ''in vitro'' study. *J Surg Res* 2001;**96**:81–89
15. Mei J, Sgroi A, Mai G, Baertschiger R, Gonelle-Gispert C, Serre-Beinier V, Morel P, Buhler LH. Improved survival of fulminant liver failure by transplantation of microencapsulated cryopreserved porcine hepatocytes in mice. *Cell Transplant* 2009;**18**:101–10
16. Machluf M, Orsola A, Boorjian S, Kershen R, Atala A. Microencapsulation of Leydig cells: a system for testosterone supplementation. *Endocrinology* 2003;**144**:4975–79
17. Sittadjody S, Saul JM, Joo S, Yoo JJ, Atala A, Opara EC. Engineered multilayer ovarian tissue that secretes sex steroids and peptide hormones in response to gonadotropins. *Biomaterials* 2013;**34**:2412–20
18. de Vos P, Bucko M, Gemeiner P, Navratil M, Svitel J, Faas M, Strand BL, Skjak-Braek G, Morch YA, Vikartovska A, Lacik I, Kollarikova G, Orive G, Poncelet D, Pedraz JL, Ansorge-Schumacher MB. Multiscale requirements for bioencapsulation in medicine and biotechnology. *Biomaterials* 2009;**30**:2559–70
19. Tendulkar S, Mirmalek-Sani SH, Childers C, Saul J, Opara EC, Ramasubramanian MK. A three-dimensional microfluidic approach to scaling up microencapsulation of cells. *Biomed Microdevices* 2012;**14**:461–69
20. Lin RY, Kubo A, Keller GM, Davies TF. Committing embryonic stem cells to differentiate into thyrocyte-like cells in vitro. *Endocrinology* 2003;**144**:2644–49
21. Khanna O, Moya ML, Opara EC, Brey EM. Synthesis of multilayered alginate microcapsules for the sustained release of fibroblast growth factor-1. *J Biomed Mater Res A* 2010;**95**:632–40
22. Darrabie MD, Kendall WJ, Opara EC. Characteristics of Poly-L-Ornithine-coated alginate microcapsules. *Biomaterials* 2005;**26**:6846–52
23. Arufe MC, Lu M, Kubo A, Keller G, Davies TF, Lin RY. Directed differentiation of mouse embryonic stem cells into thyroid follicular cells. *Endocrinology* 2006;**147**:3007–15
24. Arufe MC, Lu M, Lin RY. Differentiation of murine embryonic stem cells to thyrocytes requires insulin and insulin-like growth factor-1. *Biochem Biophys Res Commun* 2009;**381**:264–70
25. Antonica F, Kasprzyk DF, Opitz R, Iacovino M, Liao XH, Dumitrescu AM, Refetoff S, Peremans K, Manto M, Kyba M, Costagliola S. Generation of functional thyroid from embryonic stem cells. *Nature* 2012;**491**:66–71
26. Bell E, Moore H, Mitchie C, Sher S, Coon H. Reconstruction of a thyroid gland equivalent from cells and matrix materials. *J Exp Zool* 1984;**232**:277–85
27. Toda S, Sugihara H. Reconstruction of thyroid follicles from isolated porcine follicle cells in three-dimensional collagen gel culture. *Endocrinology* 1990;**126**:2027–34
28. Toda S, Koike N, Sugihara H. Thyrocyte integration, and thyroid folliculogenesis and tissue regeneration: perspective for thyroid tissue engineering. *Pathol Int* 2001;**51**:403–17
29. Arauchi A, Shimizu T, Yamato M, Obara T, Okano T. Tissue-engineered thyroid cell sheet rescued hypothyroidism in rat models after receiving total thyroidectomy comparing with nontransplantation models. *Tissue Eng Part A* 2009;**15**:3943–49
30. Whitesides GM. The origins and the future of microfluidics. *Nature* 2006;**442**: 368–73
31. Beebe DJ, Mensing GA, Walker GM. Physics and applications of microfluidics in biology. *Annu Rev Biomed Eng* 2002;**4**:261–86
32. de Jong J, Lammertink RG, Wessling M. Membranes and microfluidics: a review. *Lab Chip* 2006;**6**:1125–39
33. Lim F, Sun AM. Microencapsulated islets as bioartificial endocrine pancreas. *Science* 1980;**210**:908–10
34. Lee KY, Mooney DJ. Alginate: properties and biomedical applications. *Prog Polym Sci* 2012;**37**:106–26
35. Wu TJ, Huang HH, Hsu YM, Lyu SR, Wang YJ. A novel method of encapsulating and cultivating adherent mammalian cells within collagen microcarriers. *Biotechnol Bioeng* 2007;**98**:578–85
36. Burdick JA, Prestwich GD. Hyaluronic acid hydrogels for biomedical applications. *Adv Mater* 2011;**23**:H41–56
37. Sakai S, Hashimoto I, Tanaka S, Salmons B, Kawakami K. Small agarose microcapsules with cell-enclosing hollow core for cell therapy: transplantation of ifosfamide-activating cells to the mice with preestablished subcutaneous tumor. *Cell Transplant* 2009;**18**:933–39
38. Sakai S, Ito S, Kawakami K. Calcium alginate microcapsules with spherical liquid cores templated by gelatin microparticles for mass production of multicellular spheroids. *Acta Biomater* 2010;**6**: 3132–37
39. Oh MJ, Ryu TK, Choi SW. Hollow polydimethylsiloxane beads with a porous structure for cell encapsulation. *Macromol Rapid Commun* 2013;**34**:1728–33
40. Sakai S, Kawakami K. Both ionically and enzymatically crosslinkable alginate-tyramine conjugate as materials for cell encapsulation. *J Biomed Mater Res A* 2008;**85**:345–51
41. Santos E, Zarate J, Orive G, Hernandez RM, Pedraz JL. Biomaterials in cell microencapsulation. *Adv Exp Med Biol* 2010;**670**:5–21
42. Rowley JA, Madlambayan G, Mooney DJ. Alginate hydrogels as synthetic extracellular matrix materials. *Biomaterials* 1999;**20**:45–53
43. Lee KY, Mooney DJ. Hydrogels for tissue engineering. *Chem Rev* 2001;**101**:1869–79

44. West ER, Xu M, Woodruff TK, Shea LD. Physical properties of alginate hydrogels and their effects on in vitro follicle development. *Biomaterials* 2007;**28**:4439–48
45. Stabler CL, Sambanis A, Constantinidis I. Effects of alginate composition on the growth and overall metabolic activity of betaTC3 cells. *Ann N Y Acad Sci* 2002;**961**:130–33
46. Ye Z, Mahato RI. Emerging trends in cell-based therapies. *Preface.* Adv Drug Deliv Rev 2008;**60**:89–90
47. Orive G, Tam SK, Pedraz JL, Halle JP. Biocompatibility of alginate-poly-L-lysine microcapsules for cell therapy. *Biomaterials* 2006;**27**:3691–700
48. Coates EE, Riggin CN, Fisher JP. Matrix molecule influence on chondrocyte phenotype and proteoglycan 4 expression by alginate-embedded zonal chondrocytes and mesenchymal stem cells. *J Orthop Res* 2012;**30**:1886–97
49. Tam SK, Bilodeau S, Dusseault J, Langlois G, Halle JP, Yahia LH. Biocompatibility and physicochemical characteristics of alginate-polycation microcapsules. *Acta Biomater* 2011;**7**:1683–92
50. Lissitzky S, Fayet G, Giraud A, Verrier B, Torresani J. Thyrotrophin-induced aggregation and reorganization into follicles of isolated porcine-thyroid cells. 1. Mechanism of action of thyrotrophin and metabolic properties. *Eur J Biochem* 1971;**24**:88–99
51. Williams DW, Wynford-Thomas D. Human thyroid epithelial cells. *Methods Mol Biol* 1997;**75**:163–72

(Received June 5, 2016, Accepted September 7, 2016)